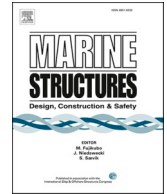




ELSEVIER

Contents lists available at ScienceDirect

Marine Structures

journal homepage: www.elsevier.com/locate/marstruc

Optimal design of offshore jacket platform using enhanced colliding bodies optimization algorithm

Naser Shabakhty^{a,*}, Alireza Asgari Motlagh^{a,b}, Ali Kaveh^a

^a School of Civil Engineering, Iran University of Science and Technology, Tehran, Iran

^b School of Civil, Mining, Environmental and Architectural Engineering, University of Wollongong, Wollongong, NSW 2522, Australia

ARTICLE INFO

Keywords:

Offshore structures
Jacket platforms
Structural optimization
Enhanced colliding bodies optimization (ECBO)
Genetic algorithm (GA)

ABSTRACT

Given the considerable volume of materials used in jacket platforms, structural optimization of these structures is always of interest. In the design optimization of offshore jacket platforms, the objective function is iteratively evaluated through a number of complex and time-consuming analyses making the optimization process computationally expensive. To reduce the computational costs, therefore, it is imperative to investigate efficient optimization algorithms with a high convergence rate to achieve optimal solutions for offshore jacket structures as a large-scale and complex problem. Accordingly, this research studies the application of a novel metaheuristic algorithm called Enhanced Colliding Bodies Optimization (ECBO) for the design optimization of a real jacket platform, SPD19A. The optimization constraints comprise stress and buckling in the members, horizontal displacements at the working point, and structural adequacy control of connections. The optimization results are subsequently compared to a design optimized by the Genetic Algorithm (GA), as an example, to evaluate the efficiency of the ECBO algorithm for the offshore jacket structure. The outcomes indicate that ECBO optimizes the jacket more effectively by 15%, while the optimization ratio of GA is 11%. Hence, the results confirm that ECBO has great and favorable efficiency and can potentially escape from local optima to reach a better design for the jacket structure.

Nomenclatures

A	The cross-sectional area of the member
C_D	Hydrodynamic coefficient of drag
C_M	Hydrodynamic coefficient of inertia
C_m	Bending term coefficient in the interaction formula
D_o, D	The outer diameter of the tubular members
F_a	Allowable axial compressive stress
F_b	Allowable bending stress
F_v	Allowable shear stress
F_{vt}	Allowable torsional shear stress
F_y	Yield stress
F_{yb}	Yield strength of the brace member
F_{yc}	Yield strength of the chord member

(continued on next page)

* Corresponding author.

E-mail address: shabakhty@iust.ac.ir (N. Shabakhty).

<https://doi.org/10.1016/j.marstruc.2024.103640>

Received 13 November 2023; Received in revised form 13 April 2024; Accepted 26 May 2024

Available online 8 June 2024

0951-8339/© 2024 Elsevier Ltd. All rights are reserved, including those for text and data mining, AI training, and similar technologies.

(continued)

F'_e	Euler buckling stress
f	Nominal axial, in-plane bending, or out-of-plane bending stress in the brace
f_a	Axial stress
f_b	Bending stress
f_{bx}	Bending stresses about the local X-axis
f_{by}	Bending stresses about the local Y-axis
f_v	Resultant shear stress due to shear force
f_{vt}	Resultant shear stress due to torsion
g_a	Allowable stress or horizontal deflection
g_i	Calculated stress or horizontal deflection
H	The height of the platform
I_p	Polar moment of inertia
$iter$	The iteration number
$iter_{max}$	Total number of iterations
M_t	Torsional moment
m	Specified mass of each colliding body (CB)
n	Number of colliding bodies
nc	Total number of constraints
pro	A parameter for regenerating a component of each colliding body (CB)
Q_f	A factor to account for the presence of nominal longitudinal stress in the chord
Q_q	A factor to account for the effects of loading type and geometry
R_p	Coefficient of the exterior penalty function
t	Thickness of the tubular members
U	Uniform flow velocity
U_w	Mean wind speed
UC	Unity Check ratio
u	horizontal velocity of the water particle inside the wave
\dot{u}	horizontal acceleration of the water particle inside the wave
V	Transverse shear force
W_p	Weight of the jacket platform
X, CB	Colliding body
x	The previous position of colliding body
x^0	The initial solution vector of each colliding body (CB)
x_{min}, x_{max}	The lower and upper bounds of design variables
x^{new}	The new position of the colliding body
$\beta, \gamma, \theta, \tau$	Joint geometry parameters
$\Delta_{X,Y}$	Horizontal deflections in X and Y directions
ϵ	The coefficient of restitution (COR)
v	The velocity of the stationary and moving bodies before collision
v_p	Acting punching shear
v_{pa}	Allowable punching shear stress
v'	The velocity of the stationary and moving bodies after collision
ρ	Water density
Φ, fit	Fitness function

1. Introduction

Steel jacket platforms are huge steel-framed structures used to explore and extract oil and gas from the deep ocean. Despite the popularity of steel jacket platforms for the oil and gas industry –about 95% of offshore platforms in the world are using jacket platforms [1]– these structures are constructed with a considerable volume of materials and, therefore, optimization of steel jacket structures has become of interest to researchers. However, the optimization of the jacket structures is acquired by analyses of these structures during several iterations. Due to the complexity and considerable time required to analyze these structures, the optimization process is often expected to become time-consuming and uneconomical.

Due to the importance of optimization in the offshore industry, numerous studies have been conducted to optimize different offshore structures [2–4]. Recently, different algorithms, such as the Cyclical Parthenogenesis Algorithm (CPA) [5], Particle Swarm Optimization Algorithm (PSO) [6], and Genetic Algorithm [7], have been applied to optimize the offshore jacket structures. Genetic Algorithm has always been of interest to researchers and engineers as a powerful tool for designing and optimizing marine structures [8,9]. Using the GA, Motlagh et al. [10] optimized a real jacket platform by taking fatigue damage into account. However, the authors emphasized that the optimization process is time-consuming and requires more studies to reduce the time consumed for the optimization and adopt more efficient algorithms in future studies. By introducing various improvements, Schafhirt et al. [11] modified the standard Genetic Algorithm and investigated the feasibility of the approach for the optimization of offshore wind turbines with jacket support structures. Nevertheless, the model used in their study was not representative of a commercial OWT. Plus, lately, considering fatigue damages, a framework was developed to optimize the orientation and location of welds connecting the joint in a welded K-node in offshore jacket structures [12].

Besides, some studies focused on sizing optimization; Oest et al. [13] developed and implemented an efficient method for analytical gradient-based sizing optimization of a support structure for offshore wind turbines. In 2018, Sandal et al. [14] also proposed an approach for sizing optimization of jacket structures for the conceptual design of jackets for offshore wind turbines and investigated

how the optimized mass depends on the number of bays and the jacket leg distance.

Recently, by using a simple optimization process, Tabeshpour, and Fatemi [15] provided an optimum bracing configuration for offshore jacket structures. They showed that the global geometry and configuration of the braces are very effective in both strength and ductility parameters. Moreover, the wind turbine as a common offshore structure was optimized by Natarajan et al. [16]. The objective of their optimization problem was to minimize the fundamental natural frequency of the structure while subjected to frequency constraints, tower top displacement constraints, and member ultimate stress constraints. Also, during the very early design phases of jacket structures, there may be very limited information available on meteorological conditions, soil conditions, specifications, etc. Hence, Oest et al. [17] realized that numerical optimization is useful for this purpose.

On the other hand, the topology optimization of offshore structures has been of interest to many studies over recent years [18]. It was also shown that topology optimization leads to a better starting point for further designs for the jacket support structure for offshore wind turbines [19]. Abou El-Makarem et al. [20] performed a topological optimization of a standard jacket platform under earthquake loading in the Gulf of Suez. In 2021, applying the teaching learning-based optimization (TLBO) algorithm and genetic algorithm (GA), Savsani et al. [21] conducted size and topology optimization for a jacket structure.

Colliding bodies optimization (CBO) is a novel and efficient optimization algorithm developed by Kaveh and Mahdavi [22]. By using memory to save some of the best solutions, the enhanced version of CBO called Enhanced Colliding Bodies Optimization (ECBO) was developed and utilized for discrete and continuous structural design problems [23]. In 2016, an optimum topology design was performed using the Colliding Bodies Optimization (CBO) method and its enhanced version (ECBO) for Schwedler and ribbed domes [24]. Kaveh and Ghazaan [25] also compared the capability of the CBO and ECBO by optimization of skeletal structures. Additionally, the Colliding Bodies Optimization Algorithm (CBO) and Enhanced Colliding Bodies Optimization (ECBO) were applied to optimize the jacket structures. However, the modeling and analysis of the jacket structure were not performed through specialized software for offshore structures [26,27].

On the one hand, due to the complexity of the structural analysis of offshore jacket structures, the design and optimization of these structures is a time-consuming and computationally expensive task. On the other hand, as optimization algorithms require tens, hundreds, or even thousands of objective function calls per run (that depends on the number of constraints and design variables), the computational cost of the whole optimization process may not usually be acceptable. Hence, the adoption of efficient optimization methods can considerably reduce the computational cost and time of optimization. Therefore, this research studies the application of ECBO, as a powerful and novel optimization method, for weight optimization of a real jacket platform, SPD19A. Besides, to boost the accuracy of structural analysis results, the SACS, specialized software for the design of offshore structures, is used for analyzing the SPD19A during the optimization process, an advantage rarely found in previous research. The optimization algorithm is coded via MATLAB. Furthermore, the optimization results are subsequently compared to the optimal design obtained by the Genetic Algorithm (GA) as a tried-and-true optimization algorithm, to investigate the efficiency of the ECBO algorithm for design optimization of jacket structures.

The next sections are as follows; Section 2 explains the optimization problem. Section 3 clarifies the Enhanced Colliding Bodies Optimization Algorithm (ECBO), while Section 4 describes the SPD19A platform and environmental specifications. Section 5 explains the design optimization of the jacket platform and the results, and finally, Section 6 provides the conclusion.

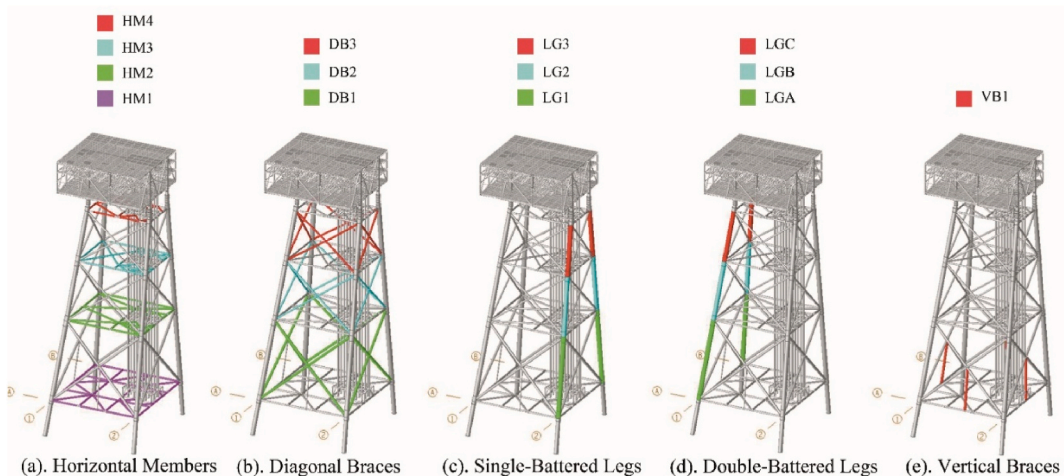


Fig. 1. The position of tubular members in each of the classified groups.

2. Optimization problem

2.1. Objective function

Considering the weight of the jacket structure as the objective function, this research aims to achieve an optimum design for the geometric properties of the sections of the jacket’s structural members. The weight of the jacket is a function of the cross-sectional geometric properties of its members and varies with the changes in the thickness and diameter of the examined members during the optimization process. It should be noted that the weight of the topside is constant during the optimization process.

2.2. Decision variables

The decision variables encompass the outer diameter (D_o) and thickness (t) of the tubular members within the jacket structure. For simplification of the problem, the primary structural members are categorized into 14 groups. Four groups of the jacket members, namely HM1, HM2, HM3, and HM4, are located in the four horizontal frames, as shown in Fig. 1(a). Three other groups of the jacket members belong to the diagonal braces, named DB1, DB2, and DB3 (Fig. 1(b)). The legs of the jacket structure form six other groups, three of which, named LG1, LG2, and LG3 (Fig. 1(c)), and the three other ones, called LGA, LGB, and LGC, whose two orthogonal sides are battered (Fig. 1(d)). The last group of the structural members is vertical braces, named VB1 and shown in Fig. 1(e). Meanwhile, the values of the outer diameter (D_o) of categorized structural members are defined in a continuous range of 30 cm–300 cm [10]. Furthermore, given the values of members’ diameter, the lower and upper boundary values of members’ thickness (t) are determined within a continuous range as described in Table 1, in accordance with the physical constraints outlined by the API code, and not taking thin-walled pipes into account by the SACS software [10]. The upper bound for thickness is merely considered to ensure that the optimization algorithm theoretically explores the entire search space of feasible and theoretical solutions and does not necessarily imply that the final optimized designs might converge to such impractical values. As the algorithm progresses through generations, unrealistic designs with excessively thick sections are naturally eliminated, and the optimized solutions converge toward more practical and realistic designs.

2.3. Design constraints

In this research, a wide range of design constraints is considered, including the control of stress and buckling in the members, displacement, and structural adequacy control of connections based on API-RP-2A code [28]. The dead and live gravitational loads, as well as environmental loads of winds, currents, and waves, are the determinant loads of the structural members of the platform. Therefore, in these members, different types of axial, shear, in-plane flexural, and out-plane flexural stresses or combinations of them are likely to form. Using the API-RP-2A-WSD [28] and AISC [29] codes, the interaction Unity Check ratios (UC) are calculated for structural tubular members. Accordingly, the amounts of stress or buckling in the members should not exceed the allowable limits defined by the equations presented in the codes. When designing cylindrical members exposed to a combination of compression and flexure, it is essential to ensure that they meet two specific criteria if the compressive stress exceeds $0.15F_a$ [28].:

$$UC = \frac{f_a}{0.6F_y} + \frac{\sqrt{f_{bx}^2 + f_{by}^2}}{F_b} \leq 1.0 \tag{1}$$

$$UC = \frac{f_a}{F_a} + \frac{C_m \sqrt{f_{bx}^2 + f_{by}^2}}{\left(1 - \frac{f_a}{F'_e}\right) F_b} \leq 1.0 \tag{2}$$

Where F'_e shows the Euler buckling stress per AISC code, and C_m is the bending term coefficient in the interaction formula dependent upon column curvature caused by applied moments [29]. Besides, f_a represents axial stress, f_b signifies bending stress, F_y stands for yield stress, f_{bx} , and f_{by} represent bending stresses about the local X-axis and local Y-axis, respectively, and finally, F_b and F_a are allowable bending and axial compressive stress, according to the AISC code [29]. When $f_a/F_a \leq 0.15$, Eq. (3) may be used for compression members in lieu of the foregoing two formulas:

$$UC = \frac{f_a}{F_a} + \frac{\sqrt{f_{bx}^2 + f_{by}^2}}{F_b} \leq 1.0 \tag{3}$$

Table 1
Decision variables.

Decision variable	Variation range	Unit	Type
Outer Diameter (D_o)	[30, 300]	cm	Cont.
Thickness (t)	$\frac{D_o}{300} \leq t \leq \frac{D_o}{2}$	cm	Cont.

Meanwhile, Eq. (4) determines the Euler buckling stress ratio for compression members [30].

$$UC = \frac{f_a}{F_e} \leq 1.0 \quad (4)$$

Eq. (5) checks the tension plus bending per API for members in tension, while Eq. (6) assesses each member for bending only [28]:

$$UC = \frac{f_a}{0.6F_y} + \frac{\sqrt{f_{bx}^2 + f_{by}^2}}{F_b} \leq 1.0 \quad (5)$$

$$UC = \frac{f_b}{F_b} \leq 1.0 \quad (6)$$

The larger amount obtained from Eq. (7) and Eq. (8) equals the shear unity check ratio [28].

$$UC = \frac{f_v}{F_v} = \frac{f_v}{0.4F_y} = \frac{\left(\frac{V}{0.5A}\right)}{0.4F_y} \leq 1.0 \quad (7)$$

$$UC = \frac{f_{vt}}{F_{vt}} = \frac{f_{vt}}{0.4F_y} = \frac{\left(\frac{M_t(D/2)}{I_p}\right)}{0.4F_y} \leq 1.0 \quad (8)$$

where f_v is resultant shear stress due to shear force, while f_{vt} stands for resultant shear stress due to torsion. Furthermore, F_v and F_{vt} , respectively, denote allowable shear stress and allowable torsional shear stress. Besides, V , A , M_t , D , and I_p are transverse shear force, cross-sectional area, torsional moment, outside diameter, and polar moment of inertia, respectively.

Moreover, it is required to control the structural adequacy of each connection. Accordingly, the maximum stress ratio based on punching shear is investigated in accordance with Eq. (9) [28]:

$$UC = \frac{v_p}{v_{pa}} \leq 1.0 \quad (9)$$

In Eq. (9), v_p is the acting punching shear, and v_{pa} is the allowable punching shear stress calculated separately for each component of brace loading and the joint type using the following equations [28]:

$$v_p = \tau f \sin \theta \quad (10)$$

$$v_{pa} = Q_q Q_f \frac{F_{yc}}{0.6\gamma} \quad (11)$$

where f is nominal axial, in-plane bending, or out-of-plane bending stress in the brace, Q_f denotes a factor to account for the presence of nominal longitudinal stress in the chord, and Q_q is a factor to account for the effects of loading type and geometry. Additionally, F_{yc} is the yield strength of the chord member at the joint, while θ , τ , and γ are joint geometry parameters, as shown in Fig. 2. Meanwhile, tubular connections are examined to ascertain the capacity of connections to bear 50% of the effective member strength of any connecting brace. The tubular joints satisfy this capability when the following condition is obtained [28]:

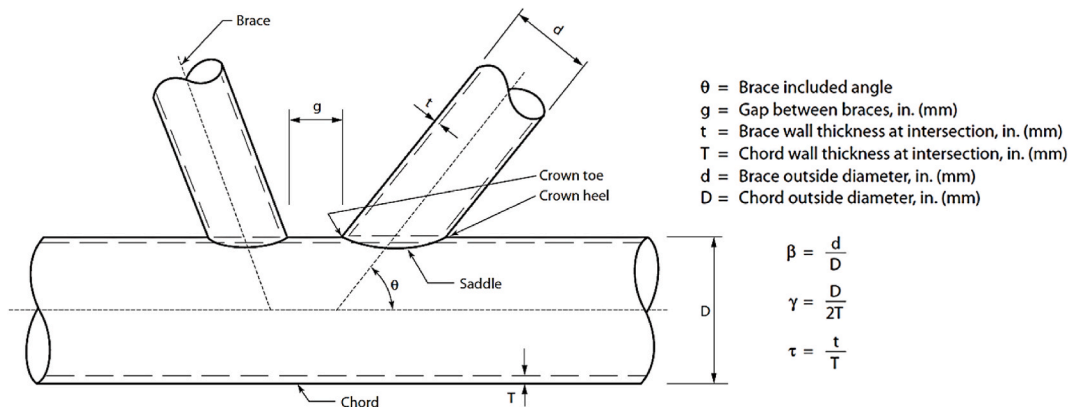


Fig. 2. Geometric parameters of tubular joints [28].

$$UC = \frac{F_{yb}(\gamma\tau \sin \theta)}{F_{yc}(11 + 1.5/\beta)} \leq 1.0 \tag{12}$$

where F_{yb} is the yield strength of the brace member, and θ , τ , γ , and β are joint geometry parameters, according to Fig. 2.

The amounts of horizontal deflections at the working point are limited to 1/200 of the platform height relative to the seabed level in both X and Y directions, as given in Eq. (13) [31]:

$$UC = \frac{(\Delta_{X,Y})_{\text{working point}}}{\left(\frac{H}{200}\right)} \leq 1.0 \tag{13}$$

Generally, the ratios of obtained values to allowable values control the constraints of the stress and buckling in the members, deflections, and punching shear in the joint connections. Accordingly, the general form of constraints in the optimization problem can be described as shown in Eq. (14):

$$UC = \frac{g_i}{g_a} \leq 1.0 \quad i = 1, 2, \dots, nc \tag{14}$$

In Eq. (14), g_a and g_i represent the allowable and calculated amount of the stress or horizontal deflection, respectively, while nc is the total number of constraints.

2.4. Fitness function

In this study, the fitness function is calculated by adding an exterior penalty function to the platform’s weight objective function. Eq. (15) indicates the relationship between the objective function, exterior penalty function, and the fitness function [7].

$$\Phi = W_p + R_p \cdot \sum_{i=1}^{nc} \left[\max\left(0, \frac{g_i}{g_a} - 1\right) \right]^2 \tag{15}$$

In Eq. (15), Φ stands for the fitness function of the problem, and W_p is the weight objective function of the platform. Moreover, g_i/g_a is associated with the design constraints thoroughly explained in Section 2.3 and signifies the maximum stress in the members or connections and the maximum horizontal deflection ratio at the working point level. R_p is the coefficient of the exterior penalty function and is constant and equal to the greatest weight of the platform for maximum values of outer diameter and thickness of all structural members of the jacket. Moreover, nc denotes the total number of constraints.

3. Enhanced colliding bodies optimization algorithm

The present research applies Enhanced Colliding Bodies Optimization (ECBO), the enhanced version of CBO developed by Kaveh et al. [23], to optimize the jacket structure. The comparison of CBO’s and ECBO’s performances has been already performed in previous research and ECBO has presented higher performances compared to CBO [25,32]. Therefore, in this research, the enhanced version of CBO is studied.

In the CBO, one object collides with another object to move toward a minimum energy level. The specified mass of each colliding body (CB), X_i , is calculated by Eq. (16) [32]:

$$m_k = \frac{1}{\frac{fit(k)}{\sum_{i=1}^n \frac{1}{fit(i)}}} \quad k = 1, 2, \dots, n \tag{16}$$

In Eq. (16), $fit(i)$ denotes the fitness function value of the i th CB, and n is the number of colliding bodies. As Fig. 3 demonstrates, according to the masses sorted in decreasing order, CBs are categorized into two equal groups: stationary and moving groups.

Moving bodies collide with stationary bodies to modify and improve their positions and push stationary objects toward better

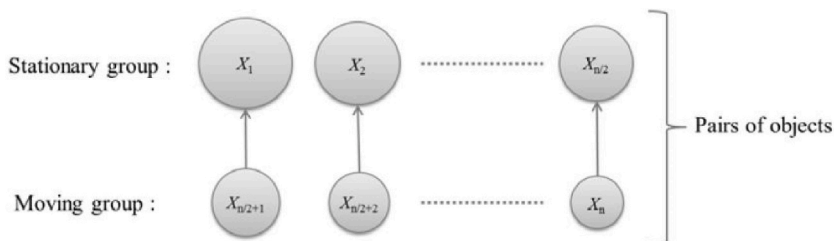


Fig. 3. The pairs of CBs for collision [32].

positions. The velocities of the stationary and moving bodies before collision (v_i) are calculated by Eq. (17) and Eq. (18), while Eq. (19) and Eq. (20) represent the velocities of the colliding bodies and after collision (v'_i) [32]:

$$v_i = 0 \quad i = 1, 2, \dots, \frac{n}{2} \tag{17}$$

$$v_i = x_{i-\frac{n}{2}} - x_i \quad i = \frac{n}{2} + 1, \frac{n}{2} + 2, \dots, n \tag{18}$$

$$v'_i = \frac{\left(m_{i+\frac{n}{2}} + \epsilon m_{i+\frac{n}{2}}\right) v_{i+\frac{n}{2}}}{m_i + m_{i+\frac{n}{2}}} \quad i = 1, 2, \dots, \frac{n}{2} \tag{19}$$

$$v'_i = \frac{\left(m_i + \epsilon m_{i-\frac{n}{2}}\right) v_i}{m_i + m_{i-\frac{n}{2}}} \quad i = \frac{n}{2} + 1, \frac{n}{2} + 2, \dots, n \tag{20}$$

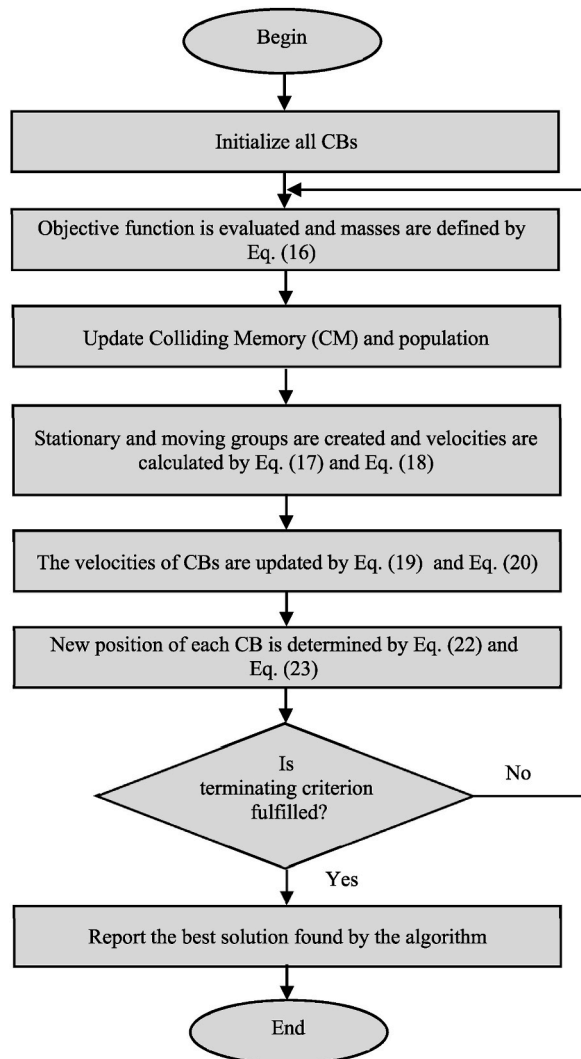


Fig. 4. The ECBO algorithm flowchart [23].

$$\varepsilon = 1 - \frac{iter}{iter_{max}} \tag{21}$$

where $iter$ and $iter_{max}$ represent the current iteration number and the total number of iterations for the optimization process, respectively. In addition, ε is the coefficient of restitution (COR). Using the following equations, new positions of each group are updated:

$$x_i^{new} = x_i + rand^{\circ} v'_i \quad i = 1, 2, \dots, \frac{n}{2} \tag{22}$$

$$x_i^{new} = x_{i-\frac{n}{2}} + rand^{\circ} v'_i \quad i = \frac{n}{2} + 1, \frac{n}{2} + 2, \dots, n \tag{23}$$

In Eq. (22) and Eq. (23), x_i^{new} , x_i and v'_i denote the new position, previous position, and the velocity after the collision of the i th CB, respectively. In addition, $rand$ indicates a random vector uniformly distributed in the range of $[-1,1]$, and the sign “ \circ ” defines an “element-by-element” multiplication.

To achieve faster and more reliable solutions for CBO, Enhanced Colliding Bodies Optimization (ECBO) is developed, which uses memory to save a number of historically best CBs and also utilizes a mechanism to escape from local optima. Fig. 4 shows the flowchart of ECBO and elaborates on the steps of this technique. In the ECBO, at the first step, the initial positions of all CBs are determined randomly in an m -dimensional search space according to Eq. (24).

$$x_i^0 = x_{min} + random^{\circ} (x_{max} - x_{min}) \quad i = 1, 2, \dots, n \tag{24}$$

where x_i^0 is the initial solution vector of the i th CB. Plus, x_{min} and x_{max} indicate the lower and upper bounds of design variables, respectively. “ $random$ ” is a random vector in the interval $[0, 1]$. In the next step, the value of mass for each CB is evaluated according to Eq. (16). In this method, to save a number of historically best CB values, colliding memory (CM) is applied. Accordingly, to produce a new generation of CBs, solution vectors held in CM are added to the population, and the worst CBs are excluded. Finally, the CBs are categorized into two groups: stationary and moving, the same as the CBO method. Moreover, the velocities of stationary and moving bodies before and after the collision are evaluated by Eqs. (17)–(20). Furthermore, the new position of each CB is calculated by Eqs. (22) and (23). Another difference between CBO and ECBO is that a parameter called “ pro ” within $(0, 1)$ is introduced in the last step. By using “ pro ”, the algorithm assesses whether a component of each CB requires change or not. For each colliding body, “ pro ” is compared with m_i ($i = 1, 2, \dots, n$), which is a random number uniformly distributed within $(0, 1)$. If $m_i < pro$, one dimension of the i th CB is selected randomly, and its value is regenerated as follows:

$$x_{ij} = x_{j,min} + random.(x_{j,max} - x_{j,min}) \tag{25}$$

In Eq (25), x_{ij} is the j th variable of the i th CB, $x_{j,min}$, and $x_{j,max}$, are the lower and upper bounds of the j th variable, respectively. It should be noted that only one dimension is changed to retain the structures of CBs. After the predefined maximum evaluation number, the optimization process is terminated. In this study, the structure of each colliding body consists of 14 pairs of continuous values indicating the outer diameter and thickness of the classified structural members of the jacket. Eq. (26) denotes the CB structure in the optimization problem.

$$CB = [D_{O_1}, t_1, D_{O_2}, t_2, \dots, D_{O_{14}}, t_{14}] \tag{26}$$

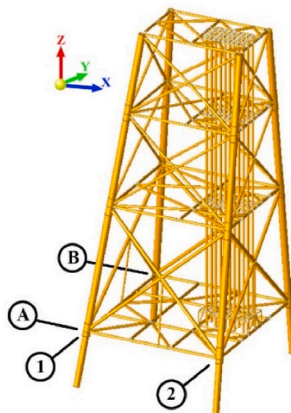


Fig. 5. Isometric view of 3D jacket model.

4. SPD19A platform and environmental specifications

The SPD19A platform is situated within the 19th phase of the South Pars field, which is positioned in the Persian Gulf. The overall dimensions of the platform deck are about 32.5 m × 27.5 m [31]. The platform model includes the weights of various equipment, such as piping, sources, instrumentation, and mechanical, electrical, safety, and firefighting equipment. The structure of the jacket is analyzed using a 3D model, shown in Fig. 5, including primary members like legs, horizontal framing, and diagonal and vertical bracings. Member groups are used to define member properties such as cross-section and material properties. The tubular members of the jacket structure are made from S355 steel plate. Moreover, the coordinates system in the model is considered in such a way that the X global axis is oriented towards platform North, the Y global axis is oriented towards platform West, and the Z global axis is pointing upward with origin at LAT.

The SPD19A platform is constructed with a four-leg jacket structure, where the legs are continuously extended and fixed into the seabed soil, reaching the fixity level. As illustrated in Fig. 6, it features a single-battered legs design on one side, with a slope of 1:7, and a double-battered legs configuration on the other side, with slopes of 1:7 and 1:8 in perpendicular directions [31]. The dimensions between the legs at the working point elevation are 24 m × 13.72 m, as demonstrated in Fig. 7 [31]. The platform's foundation consists of four piles, which are considered an extension of the legs, reaching the fixity level, and have a simple tubular cross-section. Given the soil conditions, which consist of stiff greenish clay, the fixity level of the piles is determined to be 8.5 times the outside diameter of the piles [7].

Besides, Fig. 8 demonstrates the structural elevations of the jacket structure. The structural elevations of the jacket platform comprised the working point, the top of the jacket, and the first, second, third, and fourth frames [31]. Additionally, the jacket structure's total height equals 73 m. It should be noted that the jacket members' lengths are constant during the optimization process. Furthermore, the initial weight of the SPD19A jacket platform in the original design equals 3834 tf.

Applying the finite element structural analysis software, SACS version 5.3.1.1, the jacket structure is modeled and analyzed. The structural assessment of the jacket platform is performed using in-place analysis of the structure subjected to dead and live loads as well as environmental loads caused by marine phenomena, such as waves, currents, and winds based on the platform design specifications. The in-place analysis of the jacket structure is conducted based on 100-year extreme storm conditions. The wind loads are calculated based on the API-RP-2A-WSD standard, using the 1-min mean wind speeds for 100-year extreme storm conditions provided in Table 2. The table lists the maximum wind speeds at 10 m above mean sea level for each of the eight main geographical directions specified for the project, with each data point representing the wind coming from that direction.

Accordingly, Eq. (27) calculates the wind force applied to the unit length of a tubular member [33].

$$f = \frac{1}{2} \rho C_D D_o U_w^2 \tag{27}$$

In Eq. (27), ρ is the water density, D_o denotes the outer diameter of the tubular member normal to the wind flow, U_w stands for the mean wind speed, and C_D signifies the drag coefficient.

The water depth at the location of the SPD19A platform is 64.7 m below the Lowest Astronomical Tide (LAT) level [31]. The minimum water depth for the in-place analysis is taken as LAT, while the maximum Still Water depth for the in-place analysis is equal to the sum of LAT, the Mean Higher High Water (MHHW), and 100-year Storm Surge, as furnished in Table 3.

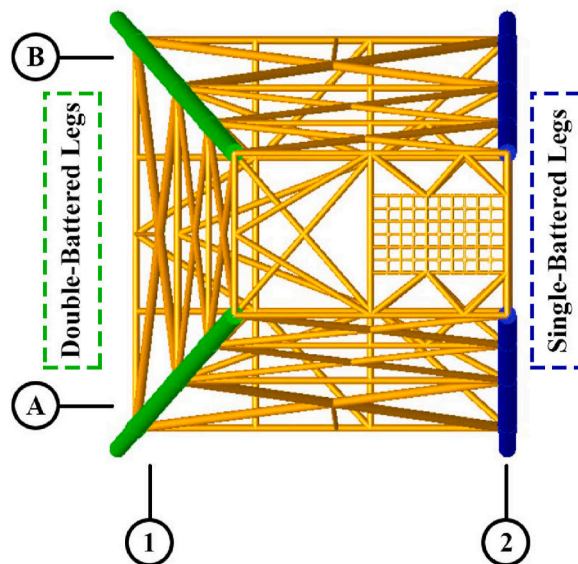


Fig. 6. Top view of the jacket structure.

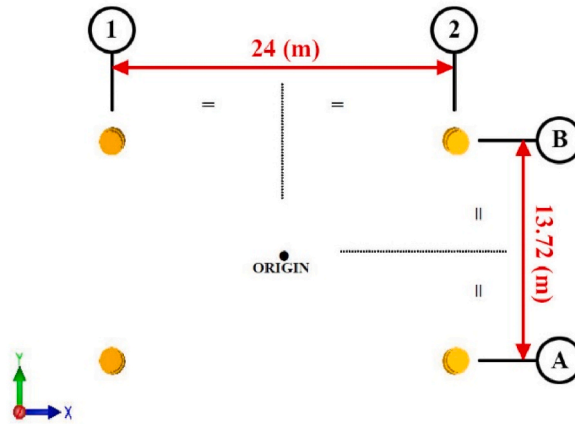


Fig. 7. Grid plan at Working Point Elev.

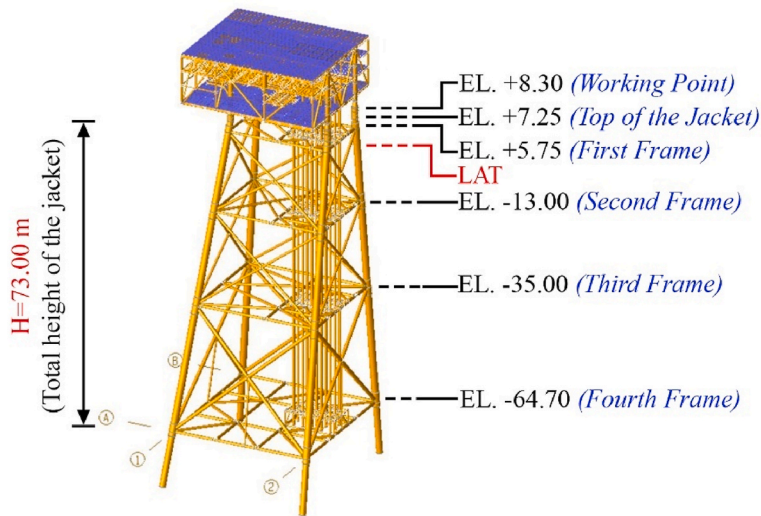


Fig. 8. Structural elevations of SPD19A platform.

Table 2
Wind data for 100-year extreme storm conditions [31].

Geographical Direction (from)	Wind Velocity (m/s)
North (N)	35.6
North East (NE)	34.9
East (E)	36.0
South East (SE)	35.2
South (S)	33.4
South West (SW)	33.0
West (W)	35.6
North West (NW)	36.7

Plus, the directional wave heights with associated periods, as well as current data for 100-year extreme storm conditions are extracted from the project specifications, shown in Tables 4 and 5, respectively [31]. Furthermore, Fig. 9 demonstrates the eight geographical directions considered for the jacket structure.

When a current is present, the total water particle velocity is modified by adding the wave particle velocity to the current velocity. If the current is inline, the magnitudes are added to give the total velocity. The wave particle velocity is computed based on the apparent wave period. In this case, the normal wave loading for a unit length of a cylindrical structure is based on the modified Morison

Table 3
100-year maximum still water depth data [31].

Parameter	Value (m)							
	N	NE	E	SE	S	SW	W	NW
LAT above Seabed	64.7							
MHHW above LAT	1.6							
100-year Storm Surge	0.1	0.1	0.2	0.3	0.2	0.1	0.2	0.3
100-year Total SWL	66.4	66.4	66.5	66.6	66.5	66.4	66.5	66.6

Table 4
Wave data for 100-year extreme storm conditions [31].

Parameter	Value							
	N	NE	E	SE	S	SW	W	NW
Wave Height (m)	9.7	8.8	10.8	11.6	10.2	8.8	10.8	12.2
Wave Period (s)	10.0	9.6	10.4	10.8	10.2	9.5	10.4	11.0

Table 5
Current data for 100-year extreme storm conditions [31].

Current (from)	Current Velocity (m/s)
Surface Current	1.28
Mid-Depth Current	1.28
1.0 m above Seabed	0.78
0.5 m above Seabed	0.71

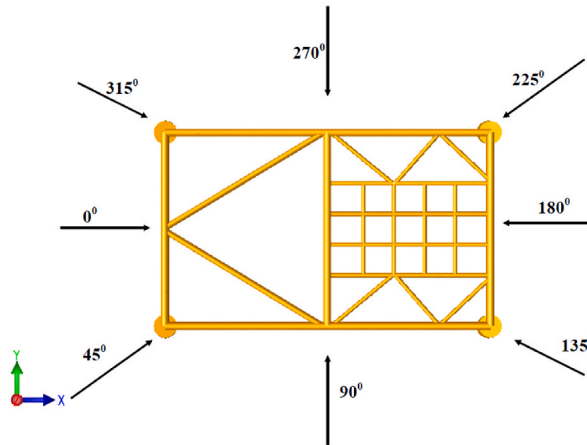


Fig. 9. Eight geographical directions for the SPD19A offshore platform [31].

equation, as shown in Eq. (28) [33].

$$f = \rho C_M \frac{\pi D_o^2}{4} \dot{u} + \frac{1}{2} \rho C_D D_o |u + U| (u + U) \tag{28}$$

where C_M and C_D , are hydrodynamic coefficients of inertia and drag, while u (m/s) and \dot{u} (m/s²) are horizontal velocity and acceleration of the water particle inside the wave, and U signifies uniform flow velocity.

5. Design optimization of SPD19A using ECBO

Lately, much research has focused on employing novel and effective approaches and algorithms for the design and optimization of marine structures [34,35]. In the same vein, this study examines the application of a continuous ECBO as a novel optimization algorithm to optimize a real jacket platform, SPD19A. The population of the first generation of the optimization process is determined

randomly. The specification of the applied ECBO algorithm is shown in Table 6. The values of colliding size memory and “pro” coefficient are considered according to the values which are recommended by Kaveh and Ghazaan [32].

Fig. 10 demonstrates the convergence curve for the optimization process of SPD19A using ECBO. Given the initial weight of the SPD19A in the original design, the ECBO reduces jacket platform weight to 3241 tf during 200 generations, leading to a 593 tf decline in the weight. The outcomes indicate the ECBO efficiently optimizes the jacket weight by a ratio of 15%.

Fig. 11 illustrates the optimization ratio in each of the classified structural members of the SPD19A platform. Regarding Fig. 11, diagonal braces are optimized more than other structural groups by 69%. Moreover, the optimization ratio for horizontal members is more significant compared to legs, while vertical braces do not have any weight reductions. Besides, Figs. 12 and 13, respectively represent the outer diameter and thickness of classified structural members, in the initial and optimum design of the SPD19A platform. Based on the findings, it can be inferred that a significant portion of the weight reduction in the optimum design is attributed to the diminished thickness of the jacket’s structural members.

Despite the lighter weight and satisfaction of all considered constraints in the optimal design, as shown in Figs. 12 and 13, the excessively large diameters and thin wall thicknesses, particularly in the high-stress regions near the seabed such as HM1 and DB1 members, are impractical and likely to lead to local failures. The excessively thin wall thicknesses of these members might result in poor fatigue performance and a high risk of cracking under cyclic wave and current loads, substantially reducing the expected service life of the jacket structure. Additionally, as illustrated in Fig. 13, the excessively diminished thicknesses of these members might provide insufficient allowance for corrosion loss over the lifetime of the structure, requiring extremely stringent corrosion monitoring and mitigation measures, which may not be practical in an offshore environment. On the other hand, the high slenderness ratios of these members make them highly susceptible to local buckling under both axial and bending loads, especially considering the external hydrostatic pressure effects near the seabed. These factors significantly increase the likelihood of premature local failures, undermining the overall structural integrity and safety of the optimized jacket design. Therefore, to ensure more practical and reliable designs, the current optimization study needs to be extended with more structural and implementation constraints, such as fatigue damage, corrosion allowance, and local buckling resistance, even if it might significantly increase the computational cost and complexity of the problem.

In the next step, as a case in point, the optimization results are compared to the design optimized by the Genetic Algorithm (GA), as a tried-and-true optimization algorithm, to evaluate the efficiency of the ECBO for offshore jacket structures. The specification of the GA used is shown in Table 7. To initiate GA optimization, the same population of the first generation of the previous optimization is used.

Regarding Fig. 14, during the same number of generations with ECBO, the GA reduces the SPD19A weight to 3395 tf, optimizing the jacket structure by 11%. Table 8 compares the optimization results of the SPD19A using GA and ECBO. Accordingly, it can be concluded that ECBO has a favorable, high convergence rate and can effectively escape from the local optimum to achieve a better design for SPD19A. Furthermore, Fig. 15 demonstrates the contribution percentage of SPD19A structural members optimized by the ECBO and GA. As shown in Fig. 15, in both ECBO and GA optimizations, the most reduction of the platform weight is caused by diagonal braces, by the ratio of 58.2% and 55.6%, respectively. Meanwhile, horizontal members have a relatively larger contribution to ECBO optimization than GA, while the contribution ratios of legs are almost equal in both. It should also be mentioned that vertical braces do not contribute to the weight reductions of the SPD19A in two optimizations.

6. Conclusion

In this study, considering various constraints, including stress and buckling in the members, horizontal displacements at the working point, and structural adequacy control of connections, a real jacket-type platform, namely SPD19A, is efficiently optimized using a metaheuristic algorithm called Enhanced Colliding Bodies Optimization (ECBO) by a ratio of 15%. The objective function is the weight of the jacket structures, while the outer diameter and thickness of the tubular members of the jacket structure are decision variables. The results indicate that a significant portion of weight reduction in the optimal design is due to the decline in the jacket structural members’ thicknesses. Moreover, according to the optimal design, diagonal braces are optimized more than other structural groups by 69%, while the optimization ratios of horizontal members and legs are 41% and 15%, respectively. It is worth mentioning that vertical braces do not have any weight reductions in the optimized design.

In addition, as an instance, another optimization is performed using the Genetic Algorithm (GA) to evaluate the efficiency of the ECBO for optimization of the SPD19A. The results show that during the same number of generations with ECBO, GA optimizes the SPD19A weight by 11%. Therefore, it can be deduced that ECBO has better competency and performance compared to GA and can effectively escape from the local optimum to attain a better design for SPD19A. Hence, due to its effective performance, ECBO can be efficiently used to reduce the computational cost of optimization of jacket structures as a large-scale and complex problem.

Furthermore, according to the optimization results, in both ECBO and GA optimizations, the diagonal braces have the most contribution to the optimization of SPD19A, by 58.2% and 55.6%, respectively. Meanwhile, horizontal members have a relatively larger contribution in ECBO optimization than GA, while the contribution ratios of legs are almost equal in both. Besides, vertical braces do not contribute to the weight reduction of SPD19A in two optimizations.

Finally, although due to the high and favorable efficiency, the application of ECBO could effectively lead to a reduction of computational costs for the optimal design of jacket structures, the structural assessment of the jacket during the optimization process is conducted using time-consuming finite element analyses. Thus, it is recommended that future research investigate the combined use of the ECBO algorithm and Machine Learning techniques for the design optimization of jacket structures to diminish the significant time and computational costs associated with finite element analyses. Besides, this research specifically focuses on investigating the

Table 6
The specifications of the applied ECBO algorithm for the optimization of the SPD19A [32].

Parameter	Value
Population size	50
Colliding memory size	2
“pro” coefficient	0.3
Stopping criterion	200 generations

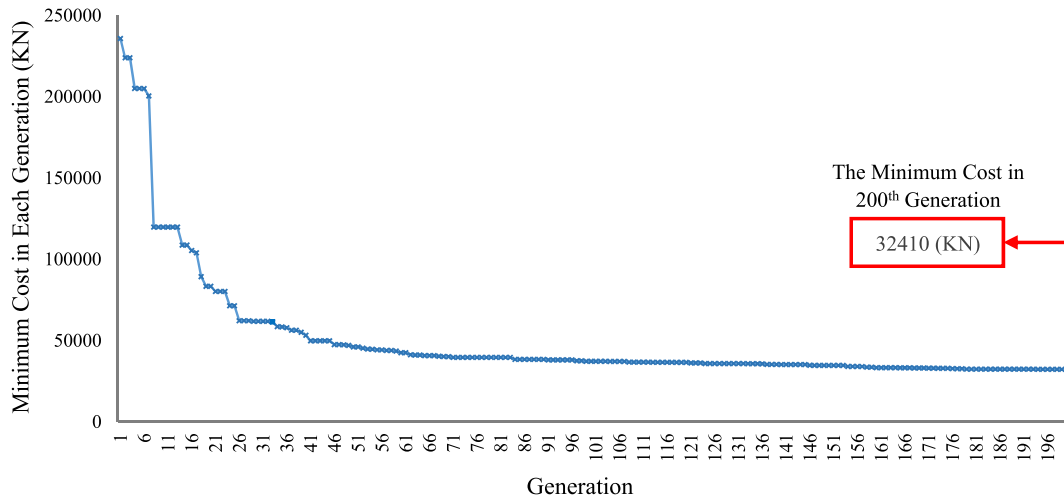


Fig. 10. The minimum cost per generation for optimization of SPD19A platform using ECBO.

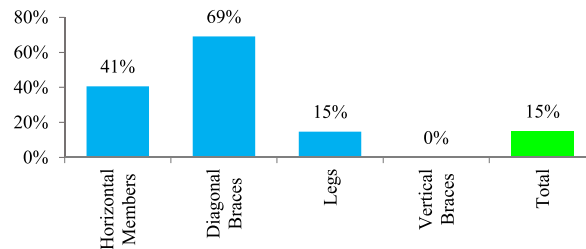


Fig. 11. The optimization ratio in each of the classified structural members of the SPD19A platform.

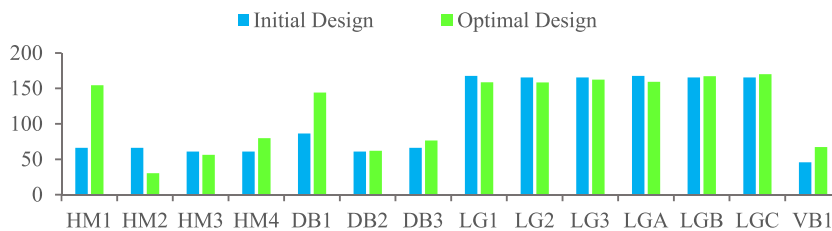


Fig. 12. The outer diameter (cm) of classified structural members in the initial and optimum design of the SPD19A platform.

performance and efficiency of an innovative ECBO algorithm for jacket platforms, using continuous variables and considering several structural constraints, in order to provide basic and preliminary insights for future studies. Therefore, for more realistic and practical designs, further research could apply discrete variables and standard structural sections, and consider a wider scope of structural constraints, such as fatigue damage estimation, corrosion allowance, earthquake considerations, as well as implementation issues.

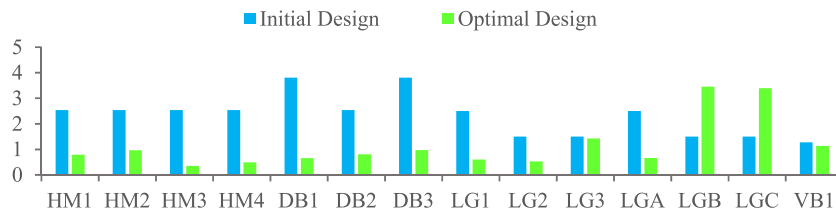


Fig. 13. The thickness (cm) of classified structural members in the initial and optimum design of the SPD19A platform.

Table 7

The specifications of the applied GA algorithm for the optimization of the SPD19A.

Genetic Algorithm [10]	
Parameter	Value or Method
Population size	50
Elite size	1
Selection	Tournament
Tournament size	2
Mate	Single point
Insertion	Complete
Stopping criterion	200 generations

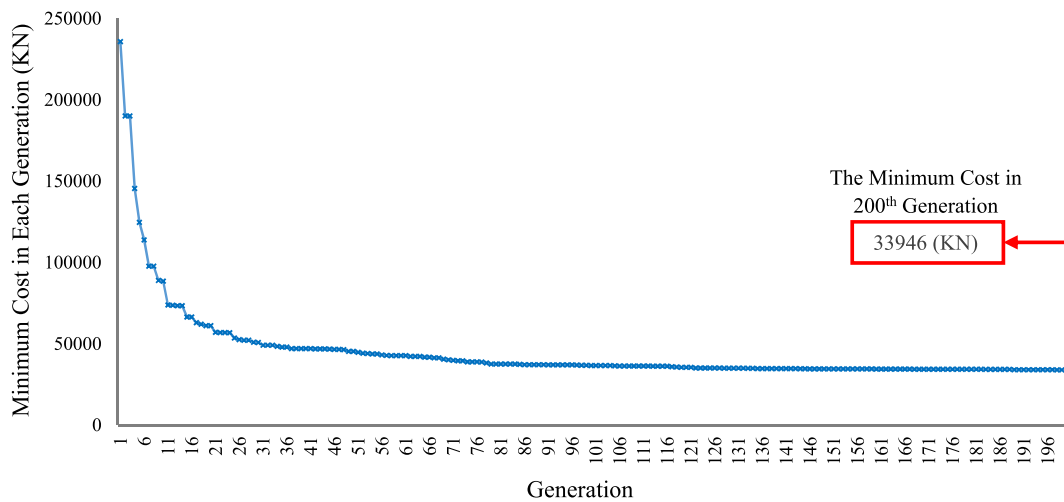


Fig. 14. The minimum cost per generation for optimization of the SPD19A platform using GA.

Table 8

The optimization results of the ECBO and GA.

	Initial weight of SPD19A (tf)	Optimized weight of SPD19A (tf)	Reduced weight of SPD19A (tf)	Optimization ratio
ECBO	3834	3241	593	15%
GA	3834	3395	439	11%

CRediT authorship contribution statement

Naser Shabakhty: Writing – review & editing, Visualization, Validation, Supervision, Project administration, Methodology, Investigation. Alireza Asgari Motlagh: Writing – original draft, Visualization, Software, Methodology, Investigation, Formal analysis, Data curation. Ali Kaveh: Validation, Supervision, Project administration, Methodology, Conceptualization.

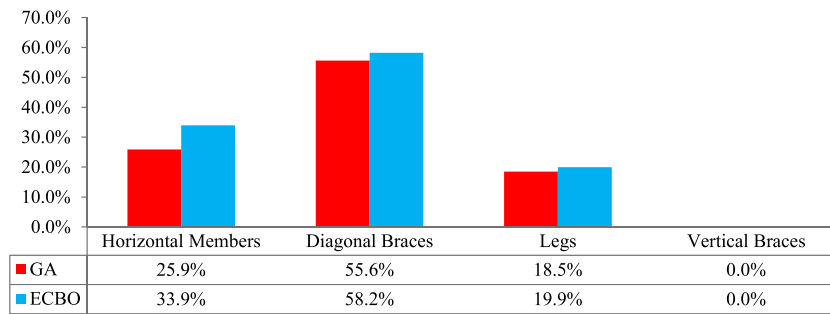


Fig. 15. The contribution percentage of the members based on structural position in the optimization processes of the SPD19A platform using ECBO and GA.

Declaration of competing interest

The authors declare that they have no known competing financial interests or personal relationships that could have appeared to influence the work reported in this paper.

Data availability

Data will be made available on request.

References

- [1] Fu F. Design and analysis of tall and complex structures. Butterworth-Heinemann; 2018.
- [2] Zhang X, Song X, Qiu W, Yuan Z, You Y, Deng N. Multi-objective optimization of tension leg platform using evolutionary algorithm based on surrogate model. *Ocean Eng* 2018;148:612–31.
- [3] Deng W, Tian X, Han X, Liu G, Xie Y, Li Z. Topology optimization of jack-up offshore platform leg structure. *J Eng Marit Environ* 2020. <https://doi.org/10.1177/1475090220928736> [Online]. Available: <https://doi.org/10.1177/1475090220928736>.
- [4] Tao J, Cao F, Dong X, Li D, Shi H. Optimized design of 3-DOF buoy wave energy converters under a specified wave energy spectrum. *Appl Ocean Res* 2021;116:102885. <https://doi.org/10.1016/j.apor.2021.102885>.
- [5] Hosseini SA, Zolghadr A. Optimization of an offshore jacket-type structure using meta-heuristic algorithms. *Int J Optim Civ Eng* 2017;7(4):565–77.
- [6] Håafele J, Rolfes R. Approaching the ideal design of jacket substructures for offshore wind turbines with a particle swarm optimization algorithm. In: *Twenty-sixth international ocean and polar engineering conference*; 2016. p. 156–63.
- [7] Nasser T, Shabakhty N, Afshar MH. Study of fixed jacket offshore platform in the optimization design process under environmental loads. *Int J Marit Technol* 2014;2:75–84 [Online]. Available: <http://ijmt.ir/article-1-289-en.html>.
- [8] Pillai AC, Thies PR, Johannung L. Mooring system design optimization using a surrogate assisted multi-objective genetic algorithm. *Eng Optim Aug.* 2019;51(8):1370–92. <https://doi.org/10.1080/0305215X.2018.1519559>.
- [9] Abyani M, Bahaari MR, Zarrin M, Nasser M. Effects of sample size of ground motions on seismic fragility analysis of offshore jacket platforms using Genetic Algorithm. *Ocean Eng* 2019;189:106326. <https://doi.org/10.1016/j.oceaneng.2019.106326>.
- [10] Motlagh AA, Shabakhty N, Kaveh A. Design optimization of jacket offshore platform considering fatigue damage using Genetic Algorithm. *Ocean Eng* 2021;227:108869. <https://doi.org/10.1016/j.oceaneng.2021.108869>.
- [11] Schafhirt S, Zwick D, Muskulus M. Reanalysis of jacket support structure for computer-aided optimization of offshore wind turbines with a genetic algorithm. In: *The twenty-fourth international ocean and polar engineering conference*; 2014. ISOPE-I-14-174, Jun. 15.
- [12] Larsen ML, Arora V, Adhikari S, Clausen HB. Optimization of welded K-node in offshore jacket structure including the stochastic size effect. *Mar Struct* 2022;82:103128. <https://doi.org/10.1016/j.marstruc.2021.103128>.
- [13] Oest J, Sørensen R, Overgaard LCT, Lund E. Structural optimization with fatigue and ultimate limit constraints of jacket structures for large offshore wind turbines. *Struct Multidiscip Optim* 2017;55(3):779–93. <https://doi.org/10.1007/s00158-016-1527-x>.
- [14] Sandal K, Verbart A, Stolpe M. Conceptual jacket design by structural optimization. *Wind Energy Dec.* 2018;21(12):1423–34. <https://doi.org/10.1002/we.2264>.
- [15] Tabeshpour MR, Fatemi M. Optimum arrangement of braces in jacket platform based on strength and ductility. *Mar Struct* 2020;71:102734. <https://doi.org/10.1016/j.marstruc.2020.102734>.
- [16] Natarajan A, Stolpe M, Njomo Wandji W. Structural optimization based design of jacket type sub-structures for 10 MW offshore wind turbines. *Ocean Eng* 2019;172:629–40. <https://doi.org/10.1016/j.oceaneng.2018.12.023>.
- [17] Oest J, Sandal K, Schafhirt S, Stieng LES, Muskulus M. On gradient-based optimization of jacket structures for offshore wind turbines. *Wind Energy Nov.* 2018;21(11):953–67. <https://doi.org/10.1002/we.2206>.
- [18] Tian X, Wang Q, Liu G, Liu Y, Xie Y, Deng W. Topology optimization design for offshore platform jacket structure. *Appl Ocean Res* 2019;84:38–50. <https://doi.org/10.1016/j.apor.2019.01.003>.
- [19] Tian X, et al. Optimization design of the jacket support structure for offshore wind turbine using topology optimization method. *Ocean Eng* 2022;243:110084. <https://doi.org/10.1016/j.oceaneng.2021.110084>.
- [20] Abou El-Makarem M, Elshafey AA, Mokhtar AA, Tork BI. Topology optimization of fixed offshore platform under earthquake loading in gulf of suez. *IOSR J Mech Civ Eng* 2019;16(1):58–71.
- [21] Savsani V, Dave P, Raja BD, Patel V. Topology optimization of an offshore jacket structure considering aerodynamic, hydrodynamic and structural forces. *Eng Comput* 2021;37(4):2911–30. <https://doi.org/10.1007/s00366-020-00983-3>.
- [22] Kaveh A, Mahdavi VR. Colliding bodies optimization: a novel meta-heuristic method. *Comput Struct* 2014;139:18–27. <https://doi.org/10.1016/j.compstruc.2014.04.005>.
- [23] Kaveh A, Ilchi Ghazaan M. Enhanced colliding bodies optimization for design problems with continuous and discrete variables. *Adv Eng Softw* 2014;77:66–75. <https://doi.org/10.1016/j.advengsoft.2014.08.003>.
- [24] Kaveh A, Rezaei M. Topology and geometry optimization of single-layer domes utilizing CBO and ECBO. *Sci Iran* 2016;23(2):535–47. <https://doi.org/10.24200/sci.2016.2137>.

- [25] Kaveh A, Ilchi Ghazaan M. A comparative study of CBO and ECBO for optimal design of skeletal structures. *Comput Struct* 2015;153:137–47. <https://doi.org/10.1016/j.compstruc.2015.02.028>.
- [26] Kaveh A, Sabeti S. Structural optimization of jacket supporting structures for offshore wind turbines using colliding bodies optimization algorithm. *Struct Des Tall Spec Build* 2018;27(13). <https://doi.org/10.1002/tal.1494> [Online]. Available:.
- [27] Kaveh A, Sabeti S. Optimal design of jacket supporting structures for offshore wind turbines using enhanced colliding bodies optimization algorithm. *Int J Optim Civ Eng* 2019;9(1):129–45.
- [28] API-Recommended practice 2A-WSD(RP 2A-WSD). twenty-first ed. 2000.
- [29] AISC. Manual of steel construction—allowable stress design. ninth ed. 1989.
- [30] SACS user's manual. Engineering dynamics. Inc.; 2010.
- [31] SPD19A structural design basis. Pars Oil and Gas Company, South Pars Gas Field Development (Phase 19) 2011.
- [32] Kaveh A, Ilchi Ghazaan M. Computer codes for colliding bodies optimization and its enhanced version. *Int J Optim Civ Eng* 2014;4(3):321–39 [Online]. Available: <https://www.sid.ir/en/journal/ViewPaper.aspx?id=417953>.
- [34] Christiansen NH, Tang BK. "Neural networks for tubular joint optimization in offshore jacket structures." Jun. 19. 2016.
- [33] Chakrabarti S. Handbook of offshore engineering. Elsevier; 2005.
- [35] Abyani M, Bahaari MR. A new approach for finite element based reliability evaluation of offshore corroded pipelines. *Int J Press Vessel Pip* 2021;193:104449. <https://doi.org/10.1016/j.ijpvp.2021.104449>.